GLOBAL GOEMETRY TECHNIQUES FOR MISSION ANALYSIS

James R. Wertz

TRW Defense and Space Systems Group
Redondo Beach, California

ABSTRACT

Geometrical procedures developed for attitude accuracy analyses and sensor bias determination can provide better physical insight and faster analysis than parametric studies of mission geometry for a wide class of problems such as:

- Attitude determination and attitude accuracy
- Sun, Moon, and Earth interference
- Eclipse conditions
- TDRS coverage
- Launch window constraints.

This paper discusses the application of inertially fixed and spacecraft fixed global geometry plots to the above groups of problems; types of problems for which these methods are and are not applicable; and specific examples of applications to spacecraft in low Earth orbit, geosynchronous orbit, and geosynchronous transfer orbit.

KEYWORDS: Global Geometry, Mission Analysis, Eclipse, Occultation, TDRS, Launch Window, Attitude Determination, Celestial Sphere

1. INTRODUCTION

This paper describes techniques for analyzing various geometrical relationships as seen by an observer located ON THE SPACECRAFT, rather than at the center of the Earth as is frequently done. The various globe plots throughout the paper are essentially drawings of a celestial globe centered on the spacecraft. The major advantage of this approach is that it provides far better physical insight into the constraints being placed on a mission analysis problem and shows the impact of major variations in these conditions. Because of this advantage, relatively simple global geometrical analyses are normally an order of magnitude faster and, consequently, far cheaper than the normal technique of automated parametric studies.

This paper is concerned with methodology rather than with specific results which have been obtained. In principle, similar results can be obtained by any of a variety of methods. In practice, however, different methodologies can produce very substantial differences in the amount of information that can be gained with a given amount of time and effort. As a single example, consider the case of a spin stabilized spacecraft for which the attitude of the spin axis is determined by measuring the angle from the spin axis to the Sun, Q, and the rotation angle about the spin axis from the Sun to the center of the Earth, U, as shown in Figure 1. Although this has been a very basic attitude technique for many years, so far as I am aware the general conditions under which the attitude solution was mathematically singular were not recognized until the introduction of the global geometry technique. At that time, the singularity conditions became obvious as discussed below and, once known, were straightforward to prove analytically (Ref. 1).

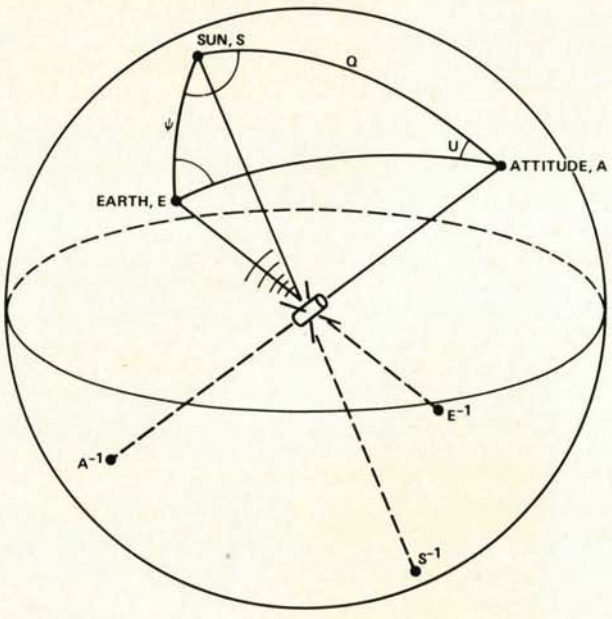

Figure 1. The spacecraft centered celestial sphere. Given the positions of the Sun and the Earth, the attitude of a spinning spacecraft can be determined by measuring the Sun angle, Q, and the Sun to Earth rotation angle, U.

Proc. Int. Symp. Spacecraft Flight Dynamics, Darmstadt, FRG, 18-22 May 1981 (ESA SP-160, Aug. 1981)

The basic approach described here was originally developed for the analysis of attitude accuracy and sensor bias determination for NASA's Goddard Space Flight Center (Ref. 1-4). However, this technique is applicable to a wide range of mission analysis problems which concern geometrical relationships over much or all of the celestial sphere. Specifically, this paper discusses the general method of undertaking a global geometry analysis, the types of problems to which it is and is not applicable, and specific applications to the following areas:

- Attitude determination and attitude accuracy studies
- Eclipse and occultation conditions
- Spacecraft to spacecraft viewing conditions
- Launch window analysis.

2. THE GLOBAL GEOMETRY TECHNIQUE

The normal method of undertaking spacecraft geometrical analyses is what, for lack of a better term, I will call "classical parametric studies." By this I mean that a straw man mission is defined, then a series of computer simulations are run to evaluate the various geometrical relations and, typically, several mission parameters are varied one or two at a time to determine how the geometry changes. Of course for any realistic number of variables this can represent an enormous expense in computer and personnel time such that only the most "interesting" variations are considered and the effect of large variations from the straw man concept are very rarely analyzed.

The alternative to this approach, which I will call global geometry analysis, is to map out, either manually or via computer aided plotting, the entire sky AS SEEN BY THE SPACECRAFT and to examine the relative geometrical relationships between all of the objects which can be sensed by the spacecraft. This "spacecraft centered celestial sphere" is illustrated in Figure 1. In order to simplify plotting, it is convenient to omit the spacecraft in the center and to plot objects on a representation of the celestial sphere of unit radius with a normal spherical coordinate system such as right ascension and declination, which is the celestial equivalent of longitude and latitude on the Earth. This is done in the remaining figures in this paper. For most purposes I have found the orthographic projections used throughout this article to be convenient. However, other projections may be useful for specific purposes, such as an Aitoff equal area plot when the relative density is the most important feature or a Mercator projection when one is computing maneuvers based on a fixed angle with respect to some reference vector such as the Sun.

To illustrate the global geometry technique, consider the very simple example of a spacecraft in an equatorial geosynchronous orbit which continuously faces the Earth and which can sense only the Earth and the Sun. The spacecraft rotates once per day about an axis which is approximately north in inertial space. A representation of the sky AS SEEN BY THE SPACECRAFT is shown in Figure 2 with a spherical coordinate system fixed relative

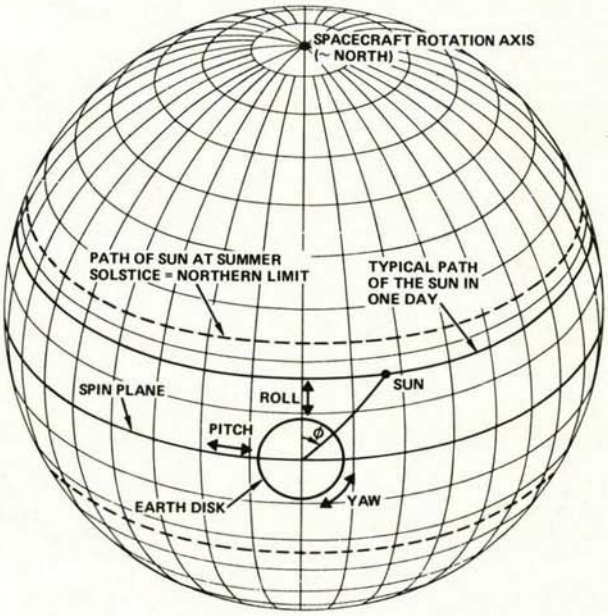

Figure 2. An "external" view of the celestial sphere as viewed by an Earth-facing spacecraft in an equatorial geosynchronous orbit (spacecraft fixed coordinates). The spacecraft yaw angle is the rotational error about the axis toward the center of the Earth and equals the difference between the predicted and measured values of ϕ.

to the spacecraft. The spin axis is at the top and the Earth, which remains fixed in spacecraft coordinates, is along the spin plane 90 degrees from the spin axis. The spacecraft rotates from west to east; i.e., such that the angular momentum vector points north. Therefore, the Sun appears to revolve from east to west in the spacecraft sky, making one revolution per day at a nearly constant angle from the spin axis. As the seasons change, the angle of the Sun above or below the spin plane oscillates between ±23 degrees, being in the spin plane (= equatorial plane) at the equinoxes. Eclipses of the Sun will occur whenever the Sun passes behind the disk of the Earth as seen from the spacecraft. As seen in Figure 2, this will occur once per day whenever the distance from the Sun to the equator is less than the angular radius of the Earth from geosynchronous orbit, 8.70 degrees. This will be between approximately February 27 and April 13 and between approximately September 1 and October 16, as can be found from any almanac. The duration of the eclipse will be just the fraction of the Sun's "orbit" covered by the Earth, or (17.4/360) x 24 hr = 70 minutes at the equinox. Times on other days can be obtained by simple spherical geometry.

Somewhat less obvious than the eclipse cycle is the measurement of roll, pitch, and yaw from the spacecraft. Roll and pitch are measured by determining the position of the Earth relative to the Earth sensor on the spacecraft. However, unless the oblateness of the Earth can be sensed (which is not necessarily impossible) the Earth sensor cannot determine yaw, which is the rotation of the spacecraft about the vector to the Earth's center. However, unless the Sun is collinear with the

Earth's center (which happens twice a day at the equinoxes) or is hidden behind the disk of the Earth, then yaw can be directly measured at any time of day by measuring the rotation of the spin axis relative to the observed position of the Sun, as shown in Figure 2. The spacecraft yaw angle is the difference between this measured angle and the predicted angle given the known geometry between the positions of the Sun, Earth, and spacecraft. This can be measured at any time of day, except for those mentioned above, by simply measuring the two components of the position of the Sun in spacecraft coordinates.

This process of numerically or analytically examining the relative geometrical relationships over the whole globe is what I mean by "global geometry analysis." On several occasions the author has used this technique to "discover" theorems about mission geometrical relationships that were previously unknown but which, when known, could then be analytically established. For example, processing of attitude data for spacecraft in geosynchronous transfer orbit at NASA's Goddard Space Flight Center has typically involved a Sun angle measurement, a nadir angle measurement, and a Sun to Earth rotation angle measurement with fixed but unknown biases permitted on each parameter. A geometrical analysis essentially similar to that above showed that under the most common conditions the Sun angle data contributed no attitude information and the rotation angle data contributed almost no information (Ref. 4). When this data was subsequently ignored in the processing, the attitude solutions remained the same, but the statistics became much more realistic.

Generally, the global geometry technique will be useful for obtaining results and improving physical insights whenever we are interested in changing geometrical relationships over a large fraction of the celestial sphere or in the impact of multiple parameters on a particular problem. Thus, this technique can prove beneficial in any of the following types of analyses:

- Attitude determination accuracy where the reference vectors can move over a large fraction of the celestial sphere (e.g., Sun, Moon, and Earth sensors or any of these in combination with star sensors)
- Attitude sensor coverage and optimum placement of sensors under the above conditions
- Attitude sensor calibration or bias determination under the same conditions
- Attitude maneuver analysis – including sensing and control strategy, interference, rhumb line maneuvers, and maneuver planning
- Eclipse and occultation conditions
- Sun or bright object avoidance conditions or geometrical constraints imposed by thermal requirements
- Spacecraft to spacecraft viewing conditions and interference from other objects
- Analysis of launch constraint conditions.

The global geometry technique will be of little benefit in problems where the geometry is essentially fixed, where variations are maintained at a sufficiently low level that linear analysis is adequate, or where the primary issue of interest is dynamics rather than kinematics. Thus, the global geometry technique will generally not be beneficial for problems such as:

- Normal (small deadband) control system analysis
- Star sensor data analysis
- Analysis of attitude dynamics.

3. APPLICATIONS

This section discusses the application of the global geometry technique to evaluating eclipse and occultation conditions, spacecraft to spacecraft viewing conditions, and launch window constraints, and summarizes the application to attitude determination analysis. References 1 to 4 contain a more detailed discussion and examples of the application of this technique to attitude and bias determination, sensor placement, and attitude maneuvers. In addition, Reference 4 contains a detailed presentation of the method of manually constructing plots such as shown here and a reference to existing subroutines for automated plot generation.

3.1 Attitude Determination Analysis

The purpose of global geometry attitude determination analyses is to determine the relative attitude accuracy which is possible for various geometrical conditions or, conversely, to determine regions of the spacecraft sky for which specified accuracy conditions can be met. Reference 4 provides a detailed discussion of both types of analyses. This section explains the basic principle of geometrical attitude analysis and identifies the geometrical criteria for mathematical singularities in attitude solutions.

Irrespective of whether the process is carried out explicitly (and it virtually never is), the general process of attitude determination for any given spacecraft axis is based on determining the locus of possible attitudes for that axis on the celestial sphere given by two or more specific measurements. The attitude estimate is then the intersection of the loci of the several measurements. For any one measurement the locus of possible attitudes consists of those points on the spacecraft centered celestial sphere which are possible spacecraft attitudes consistent with the given measurement. For example, if a measurement implies that the angle between the attitude vector and the Sun is 60 degrees, then the corresponding locus of possible attitudes on the celestial sphere consists of all points 60 degrees from the Sun, i.e., a small circle of radius 60 degrees centered on the Sun.

As an example of the attitude determination process, consider the case of determining the spacecraft spin axis by measuring the Sun angle, Q, and the rotation angle, U, from the Sun to the center of the Earth. The single axis Sun angle measurement is the simplest to visualize and implies that

the reference axis of the Sun sensor lies on a small circle on the celestial sphere of radius Q centered on the Sun. Thus, in Figure 3 the constant "latitude" lines are the loci of possible attitudes for a spacecraft axis located at any given angle from the Sun.

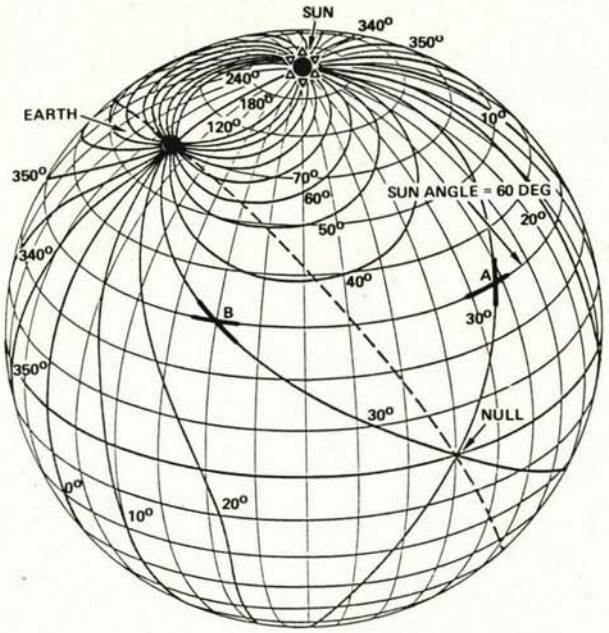

Figure 3. Loci of possible attitudes for various Sun to Earth center rotation angles for a Sun-Earth angular separation of 30 degrees (inertially fixed coordinates). The latitude lines are the loci of possible attitudes for various Sun angles. Thus, for example, a Sun angle of 60 degrees and Sun-Earth rotation angle of 30 degrees implies that the attitude will be at either point A or point B.

The loci of possible attitudes corresponding to a given rotation angle about the attitude from the Sun to the center of the Earth are considerably more complex, as illustrated in Figure 3 for a Sun-Earth separation of 30 degrees. The fact that these loci are not small circles implies that the attitude solutions do NOT behave like simple cone intersections. The spin axis attitude is now determined by finding the intersection of the appropriate loci on Figure 3. For example, for the geometry of this figure, a Sun angle of 60 degrees and a rotation angle between the Sun and the Earth of 30 degrees implies that the spacecraft atttitude is at either point A or point B. (Both solutions are consistent with the given data. Normally, other information exists to allow us to select the proper solution.)

The accuracy with which the spacecraft attitude can be determined anywhere on the celestial sphere depends on both the density of loci in that region – high density corresponds to a more accurate attitude – and on the angle at which the Sun angle and rotation angle attitude loci intersect. If the loci are nearly perpendicular, as they are between the Sun and the Earth, the attitude solutions are accurate and if the loci intersect at shallow angles then there will be a large attitude uncertainty because a small variation in either measurement would result in a large shift in the attitude. It can be seen from the figure that the lines of constant "latitude" (= Sun measurement loci) are parallel to the rotation angle loci all along the great circle through the Earth which is perpendicular to the Earth/Sun line. Thus, whenever the spacecraft attitude lies on this line, attitude solutions based on the Sun angle and the Sun to Earth rotation angle will be singular. This is the singularity condition referred to in the introduction. In addition, any attitude solution based on the Sun to Earth rotation angle measurement will have a large potential error whenever the attitude is near the point in the spacecraft sky which is perpendicular to the directions to the Earth and the Sun because of the low density of loci in this region. (This point perpendicular to the Earth/Sun great circle is labeled "null" in Figure 3.)

Although we have used a specific geometrical procedure to identify singularity conditions, these singularities will exist for any method used to compute the attitude based on the given measurements. That is, the singularity refers to the basic information content of the attitude measurement and NOT to the specific technique by which the measurements are processed. For a more extended discussion and examples of attitude and bias determination geometry see References 1 to 4.

3.2 Eclipse Conditions

This section describes the process of analyzing eclipses as seen by the spacecraft and provides an expression for the level of illumination during a partial eclipse. The general method of eclipse analysis was illustrated in the introductory example – an eclipse occurs whenever the Sun goes behind the disk of the Earth, Moon, or other object as viewed from the spacecraft. However, an additional complication arises from the finite size of the solar disk. As illustrated in Figure 4, an eclipse will be either partial, total, or annular depending on whether the Sun's disk is partially covered, totally covered, or behind, but larger than the object blocking it such that portions of the Sun's disk can be seen all around the eclipsing object. All three types of eclipses occur both on the Earth's surface, when the Moon obscures the Sun, and in space. (When the obscuring object is sufficiently small so as to block a

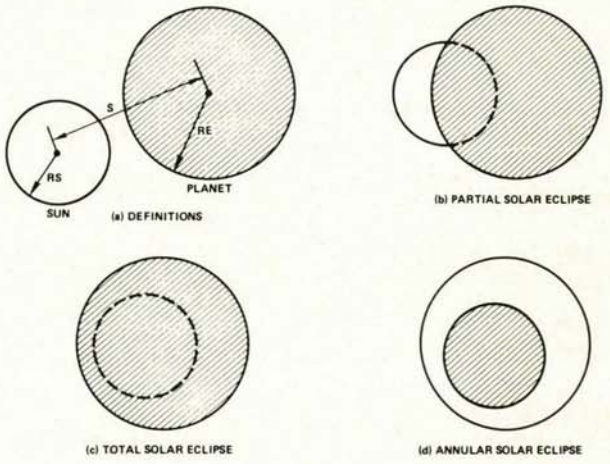

Figure 4. Solar eclipse geometry

negligible fraction of the incident light, the event is referred to as a transit rather than as an annular eclipse.)

Each total eclipse must be preceded and followed by a partial eclipse in which the light intensity is very nearly proportional to the percent of the solar disk which is obscured. A partial eclipse will occur whenever the angular separation, S, between the Sun and the center of the Earth (or other spherical obscuring object) falls in the range RE - RS < S < RS + RE, where RS and RE are the angular radii of the Sun and the Earth, respectively. A full expression for the occulted area is given in Appendix A of Reference 4, but is unnecessarily cumbersome to evaluate for normal eclipse conditions. For most practical purposes, an adequate approximation is

$$A = 0.5\ RS^2\ (2\pi - \phi + \sin\phi) \qquad (1a)$$

where A is the unocculted area of the Sun and

$$\phi = 2 \arccos [(S - RE)/RS] \qquad (1b)$$

Returning to the geometry of Figure 2, the most rapid change in illumination for our geosynchronous satellite example will occur at the equinoxes when the Sun is moving perpendicular to the disk of the Earth. At these times each partial eclipse will last 2 minutes such that the total eclipse sequence will be: full intensity — 2-minute partial eclipse — 68-minute total eclipse — 2-minute partial eclipse — full intensity.

3.3 Occultation Conditions and Spacecraft-to-Spacecraft Viewing

This section describes specific conditions under which occultations and transits will occur and discusses the motion of a spacecraft as seen from a second spacecraft. This particular problem is relevant at present because of the increase in spacecraft-to-spacecraft tracking brought about by the forthcoming Tracking and Data Relay Satellite System, TDRSS. Although the detailed relative spacecraft motion is normally quite complex, the physical insight gained from the global geometry approach allows the user to understand the sources of the motion and the impact of changes in the relative orbit parameters and to put numerical bounds on the apparent motion of a spacecraft viewed from a second spacecraft.

The general problem of occulting of portions of the celestial sphere and of Earth, Moon, or Sun avoidance can be conveniently dealt with by constructing the occulted areas on celestial sphere plots such as those shown in the figures here. This is usually most conveniently done by having the plots fixed in inertial coordinates, rather than in spacecraft coordinates as was done in Figure 2, and showing the relative motion of the Earth or other objects of interest. Examples of this type of plot are given in Figures 6 and 7 below.

A more specific problem which occurs frequently is that of the occultation of a possibly nearby object by the Earth for a spacecraft orbiting the Earth, as in the occultation of TDRS by the Earth. In this case, it is frequently convenient to consider the geometry from the perspective of the object being occulted since, of course, an occultation of an object by the Earth is equivalent to an occultation of the spacecraft by the Earth as seen from the object. Thus, we could analyze eclipses by plotting the orbit of a spacecraft as seen from the perspective of the Sun or, in a somewhat more practical example, we could determine the conditions for a total solar eclipse by examining transits of the spacecraft in front of the Earth as seen from the apex of the Earth's shadow cone.

In order to analyze viewing and occultation conditions, we need to determine the apparent shape of a spacecraft's orbit as viewed from elsewhere in space. In general, an elliptical orbit viewed from any location in space will remain elliptical when projected onto a plane, but even for a circular orbit the center of the observed ellipse is not coincident with the center of the orbit except when viewed from infinity. This is illustrated in Figure 5 for a circular spacecraft orbit viewed from nearby and above. For a circular orbit of radius R viewed at distance D from the center of the Earth and from an angle I above the orbit plane, the minor axis of the apparent ellipse will be along the line from the observer to the center of the Earth and will extend above the center of the Earth by the angle M_1 and below the center of the Earth by the angle M_2 where

$$\tan M_1 = R \sin I/(D + R \cos I) \qquad (2)$$

$$\tan M_2 = R \sin I/(D - R \cos I) \qquad (3)$$

The semimajor axis, M_j, of the apparent ellipse is given by (Ref. 5):

$$\sin^2 M_j = 2 R^2/(D^2 + R^2 + \sqrt{X}) \qquad (4a)$$

where

$$X = (D^2 + R^2)^2 - 4 D^2 R^2 \cos^2 I \qquad (4b)$$

For simplified computations note that M_j falls in the range

$$\arcsin (R/D) \geq M_j \geq \arctan (R/D) \qquad (4c)$$

which is adequately narrow for most applications.

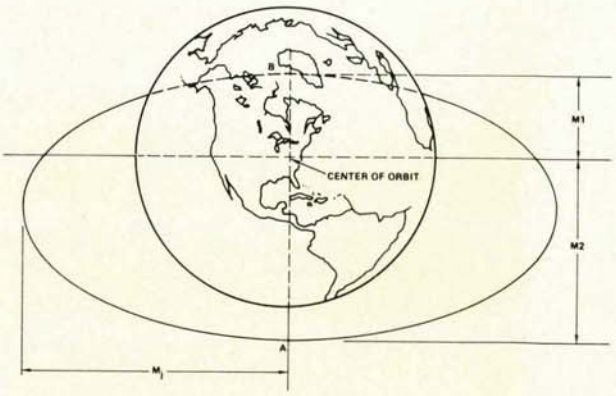

Figure 5. Appearance of a CIRCULAR orbit viewed obliquely from near point A

As can be seen from Figure 5, occultation of a spacecraft in a circular orbit can occur without transit occurring, but if a transit occurs then occultation must also occur. For a noncircular orbit the general conditions for occultation and transit are:

$RE < M_{1min}$ Neither transit nor occultation will occur.

$RE > M_{1max}$ Occultation will occur, transit may or may not occur.

$RE > M_{2max}$ and $D > A$ Both transit and occultation will occur.

where M_{1min}, M_{1max}, and M_{2max} are the minimum and maximum values of M_1 and M_2 as defined above (Ref. 4). These may be obtained by a direct extension of Equations (2) and (3) as:

$$\tan M_{1min} = P \sin I/(D + P \cos I) \quad (5a)$$

$$\tan M_{1max} = A \sin I/(D + A \cos I) \quad (5b)$$

$$\tan M_{2max} = A \sin I/(D - A \cos I) \quad (6)$$

where

P = spacecraft perifocal distance

A = spacecraft apofocal distance

D = distance from observer to center of Earth

RE = angular radius of the Earth as seen by the observer

I = inclination of spacecraft orbit relative to the observer's line of sight (i.e., 90 degrees minus the angle between the line of sight and the orbit normal)

If none of the above conditions are satisfied, then whether occultation or transit occurs will depend on the specific orientation of the observer relative to the spacecraft perigee and the orbit will need to be evaluated on a point-by-point basis.

As an example of the application of the above, consider the case of the occultation of TDRS for a spacecraft in a low Earth circular orbit. In this case, $M_{1max} = M_{1min}$, RE is the geosynchronous angular radius of the Earth, 8.70 degrees, and I is given by

$$\sin I = \sin i \sin |L_{spc} - L_{TDRS}| \quad (7)$$

where i is the inclination of the spacecraft orbit relative to the Earth's equator, L_{spc} is the longitude of the ascending node of the spacecraft at the time in question, and L_{TDRS} is the TDRS longitude. Because $M_{1min} = M_{1max}$, Equation (5) becomes an absolute condition on whether or not occultation will occur. In addition, for a circular orbit, the condition $RE > M_{2max}$ becomes an absolute condition on whether transit will occur. (Note that in this case transit refers to passage of the spacecraft in front of the disk of the Earth as seen by TDRS.) Since I oscillates over the range 0 to i as L_{spc} rotates about the Earth, Equation (5) can be used to determine on which orbits either of the TDRS spacecraft will be occulted without having to generate sample orbits for point-by-point testing.

Irrespective of the occultation conditions above, it may be of interest to determine the actual path of a spacecraft on the celestial sphere as seen by a second spacecraft, as in the case of TDRS tracking by a low orbiting spacecraft. For concreteness, we will consider the case of a spacecraft in a 3000-km circular orbit with an inclination of 34 degrees as illustrated in Figure 6. The heavy solid line from lower left to upper right is the "orbit of the Earth" on the celestial sphere as seen by the spacecraft. The two dashed lines parallel to the Earth's orbit are the envelope of the disk of the Earth as it moves across the sky. Thus, the two caps around each pole outside the dashed lines are the regions of the celestial sphere never occulted by the Earth for this orbit. (The expression for the envelope of the Earth's disk for a noncircular orbit is given below in the launch window discussion.)

The line labeled "Ecliptic" is the annual path of the Sun as seen by either the Earth or the spacecraft. The autumnal equinox of approximately September 22 occurs as the Sun crosses the equator from north to south directly below the center of the figure. The maximum duration eclipse will occur when the Sun crosses the orbit plane. We see from the figure that, for the orbit illustrated, this occurs at a declination of about 14 degrees (or -14 degrees for the crossing on the other half of celestial sphere not shown in Figure 6). From any astronomical ephemeris we find that this occurs on approximately August 15 (or February 12 for the other crossing). Similarly, the summer/fall eclipse season ends when

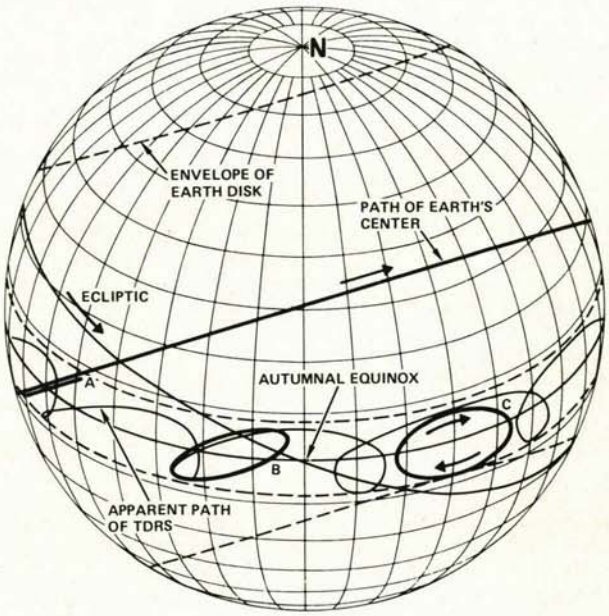

Figure 6. Celestial sphere as seen by a spacecraft in 3000 km circular 34 degree inclination orbit showing the apparent motion of the Earth, Sun, and TDRS spacecraft (inertially fixed coordinates). See text for discussion.

the Sun crosses the envelope of the disk of the Earth at a declination of -9 degrees on about October 17. At this time, the Sun will remain uneclipsed for several months before the next eclipse season begins on the opposite side of the celestial sphere from Figure 6.

The motion of a second spacecraft in the sky is substantially more complex than that of the Earth or Sun because it is the sum of the motion of the two spacecraft. This will of course be familiar to those who are astronomically oriented as equivalent to the apparent path of any of the outer planets relative to the Earth. Again using TDRS as an example, we can subdivide the relative motion on the sky into components due to the motion of the low orbiting spacecraft and that due to the 24-hour orbit of TDRS itself. If we first ignore the motion of TDRS in its orbit, then its apparent path on the sky due to the motion of the low orbiting spacecraft will be just the mirror image of the motion of the spacecraft as seen by TDRS. As discussed above, this will be an ellipse whose major axis is parallel to the plane of the "orbit" of the Earth as seen by the spacecraft. Three representative ellipses are indicated by A, B, and C on Figure 6. (Compare with Figure 5 and Equations (2) to (4).) The apparent position of TDRS will travel along the ellipse with a period equal to the spacecraft orbital period, or about 2.5 hours for our example.

Superimposed on the above motion will be the motion of TDRS itself which will carry the center of the apparent elliptical path around the celestial sphere in 24 hours. The net motion is a looping apparent path shown by the light solid line in Figure 6. From Equation (3), the maximum apparent distance of TDRS from the equator will be 8.67 degrees. Thus, the rather complex motion of TDRS will be confined within a band of ±8.67 degrees of the equator as shown by the dotted lines on the figure. This band could be narrowed somewhat by inclining it slightly relative to the equator to account for the reduced foreshortening on the far side of the orbit as given by Equation (2).

3.4 Launch Window Analysis

The normal technique for examining multiple launch window constraints is to block out unallowed regions for each constraint on a plot of date versus time of day and then to examine the plot to see if any window remains. This is an appropriate approach for looking exclusively at the launch window itself, but is very unsatisfactory for mission analysis in that it doesn't supply physical insight into either the causes of the constraints or how major changes in them would affect the launch window. An alternative which provides the requisite physical insight is to plot the necessary conditions as constraints on the placement of the orbit ON THE CELESTIAL SPHERE so that the impact of each constraint can be examined directly.

To examine the global geometry approach and contrast it with the usual technique, let us consider the example of a spacecraft in a 24-degree inclination geosynchronous transfer orbit and initially require that throughout the orbit the Sun remain within 23 degrees of the orbit plane in order to maintain thermal conditions no worse than on station, and that there be no eclipse throughout the transfer orbit so that continuous power and yaw sensing are provided. Is this a reasonable set of constraints? Does it provide an adequate launch window throughout the year? What is the impact of changing the orbit inclination? How do these constraints relate to those in a low Earth parking orbit or in the initial geosynchronous orbit?

Figure 7 shows the geometry for the above example in the usual global geometry format. Again the Earth's orbit as seen by the spacecraft is the heavy solid line from upper left to lower right and the dashed line is the envelope of the Earth's disk as the spacecraft moves in its highly elliptical orbit. This envelope is most easily plotted by determining for various points along the orbit the average radius of the Earth, ρ, and the angle, θ, between the orbit plane and the direction to the envelope at that point, as shown in Figure 8. θ is given by:

$$\theta = \arccos(\Delta\rho/\Delta\nu) \qquad (8)$$

where $\Delta\rho$ is the change in angular radius of the Earth, ρ (= arc sin RE/D), over a small change in true anomaly, $\Delta\nu$. Note that the argument of perigee is determined in Figure 7 by requiring that apogee occur on the equator. A second essentially identical plot could be prepared for apogee at the ascending node. Our requirement for no eclipse during the transfer orbit implies that the Sun must be outside the dashed line in Figure 7. Our second requirement of having the Sun within ±23 degrees of the orbit plane implies that it must lie within the light solid line parallel to the Earth's orbit. In addition, the Sun never ranges further than ±23.5 degrees from the equator, so this condition is also marked on the plot.

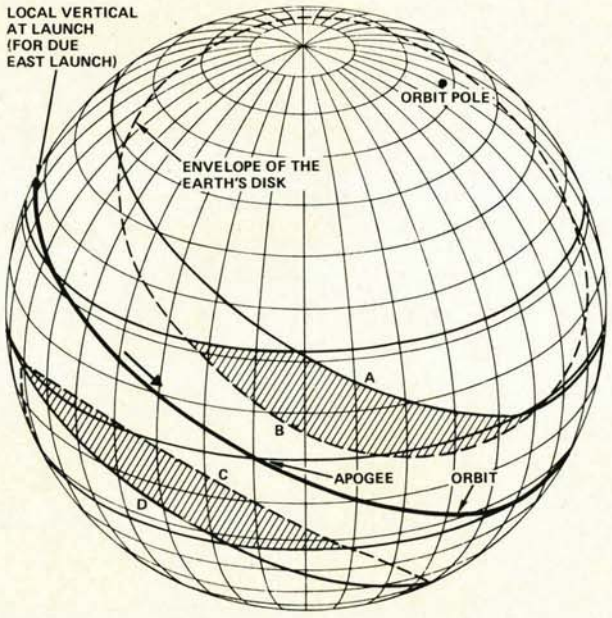

Figure 7. Celestial sphere as seen by a spacecraft in geosynchronous transfer orbit showing the possible positions for the Sun which are within ±23 degrees of the orbit plane, but for which no eclipse occurs during the transfer orbit (inertially fixed coordinates)

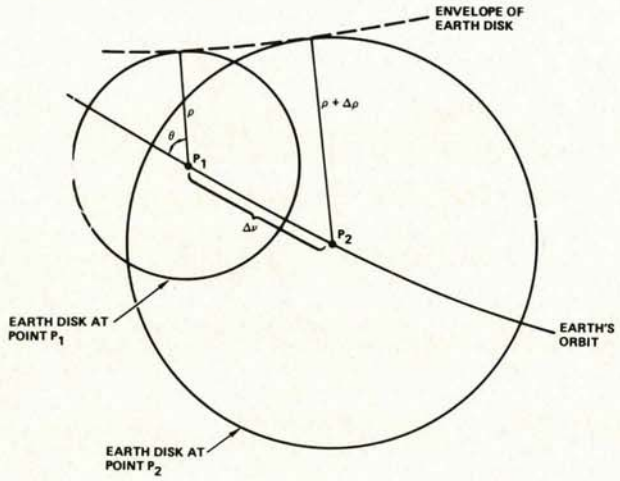

Figure 8. Geometry and parameter definitions for computing the envelope of the Earth's disk

The declination of the Sun on our plot will be a function of the launch date. Our various conditions on the transfer orbit imply that for any given date (and, therefore, declination of the Sun) we must adjust the right ascension of the ascending node of the spacecraft orbit (and, therefore, the launch time) such that the Sun falls within the shaded region. Because the shaded area covers all possible declinations, a launch window is available at all times of the year. Further, the minimum width of the launch window will be about 24 degrees (= 96 minutes) at the solstices. When the Sun is within about 3 degrees of the equator (from approximately March 13 to 28 and September 15 to 30) there will be two launch windows per day.

In addition to the above results, which could equally be read from a more normal launch window plot, Figure 7 makes clear what the general impact would be of changing any of the constraints. For example, increasing the transfer orbit inclination would narrow the window slightly, but would have no other significant effect. However, decreasing the inclination by more than a few degrees would eliminate the launch window at the equinoxes. If it is our intent to use the Sun as a yaw reference for a motor firing at apogee, then a potential basic problem is immediately apparent since for the conditions we have set out the Sun will be within approximately 30 degrees of the Earth's center except when launch occurs near the time of the equinoxes. This implies either a potentially more stringent accuracy requirement for the yaw Sun sensor or some change in mission planning. Requirements for other mission phases can be examined by plotting the other relevant orbits directly on Figure 7.

We may transform Figure 7 into the more usual launch window plot by determining the launch times associated with a given right ascension of the ascending node, RANODE, relative to the Sun according to:

$$\text{RANODE} = \text{RA(launch site)} + 270 \text{ deg} \quad (9a)$$

$$= \text{EL} + \text{GST} + 270 \text{ deg} \quad (9b)$$

where RA(launch site) is the instantaneous right ascension at launch, EL is the east longitude of the launch site, and for simplicity we have assumed a due east launch. (A different launch azimuth would affect only the constant 270 degree term.) The Greenwich Sidereal Time, GST, measures the angular orientation of the Earth in inertial space and is related to Universal Time, UT (expressed in degrees), by

$$\text{GST} = 99.6910 \text{ deg} + 36000.7689\ T + \text{UT} \quad (10)$$

where T is time since noon UT on January 0, 1900 (= Jan. 0.5, 1900) in units of Julian centuries of 36,525 days and a term in T^2 has been omitted. (For a further discussion of sidereal time and other relevant expressions, see, for example, Reference 4 Appendix J.) From the above, the Universal Time for a given right ascension and date is

$$\text{UT} = [(\text{RANODE} - \text{EL} - 270 \text{ deg} - 99.691 \text{ deg} - 0.985647335\ \Delta D)\ \text{Mod}_{360}]/1.002737909 \quad (11)$$

where ΔD (= Julian Date - 2,415,020) is the number of days from January 0.5, 1900, to 0 hr UT on the day in question and all other quantities are in degrees.

Figure 9 shows the results of transforming the regions of Figure 7 to a more normal launch window plot. The four limiting curves have been labeled A, B, C and D on both plots for comparison. While Figure 9 is convenient for launch window timing, it does not provide the direct physical insight appropriate to undertaking mission analysis or examining the impact of possible variations in the launch constraints.

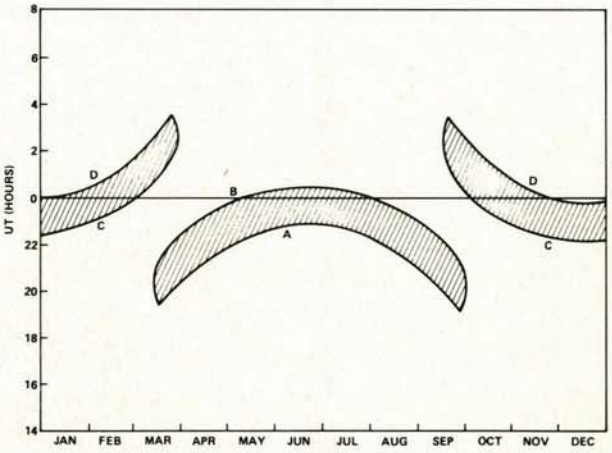

Figure 9. Typical plot of launch window availability for the conditions of Figure 7. Curves A, B, C, and D correspond to curves with the same labels on Figure 7.

4. DISCUSSION

The example above illustrates the major advantages of the global geometry approach to mission analysis. The principal advantage is that it provides a direct physical insight into spacecraft geometry

problems, and, consequently, helps the mission analyst understand the causes and impact of various conditions and, equally important, the impact of varying the mission conditions. This understanding of the spacecraft geometry helps to ensure optimal solutions to mission problems and verify that proposed solutions are based on sound engineering judgment rather than partial parametric studies.

In addition, global geometry studies can normally be undertaken in a matter of hours rather than the days or weeks frequently required for the more complex parametric analyses. This means both greatly reduced cost and the potential for using such studies at an earlier phase of mission development to ensure that the general direction of planning is reasonable and that superior solutions have not been inadvertently bypassed.

Global geometry techniques should supplement rather than replace the more traditional analyses. Detailed parametric studies are critical in the later stages of mission development to "fine tune" mission and hardware parameters. However, they should be augmented by simpler, faster techniques for preliminary mission analysis or whenever a clear physical insight is missing.

Finally, I would like to thank R.F. Brodsky and Landis Markley for their very helpful suggestions and comments.

5. REFERENCES

1. Wertz J R & Chen L C 1975, Geometrical Procedures for the Analysis of Spacecraft Attitude and Bias Determinability, Paper No. AAS75-047, AAS/AIAA Astrodynamics Specialist Conference, Nassau, Bahamas, July 28-30, 1975.

2. ----, Geometrical Limitations on Attitude Determination for Spinning Spacecraft, *J Spacecraft*, Vol. 11, pp 564-571.

3. Chen L C & Wertz J R 1977, Single-Axis Attitude Determination Accuracy, AAS/AIAA Astrodynamics Conference, Grand Teton National Park, Wyoming, September 7-9, 1977.

4. Wertz J R (ed) 1978, *Spacecraft Attitude Determination and Control*, Dordrecht, D Reidel Publishing Co.

5. Markley L, private communication.